Fabrication by Annealing at Approximately 1030°C and Electrical Characterization of Lead-Free $(1-x)Bi_{0.5}K_{0.5}TiO_3$–$xBa(Fe_{0.5}Nb_{0.5})_{0.05}Ti$(Piezoelectric Ceramics

N. Truong-Tho & N. T. Nghi-Nhan

Journal of Electronic Materials

ISSN 0361-5235
Volume 46
Number 6

Journal of Elec Materi (2017)
46:3585-3591
DOI 10.1007/s11664-017-5396-x

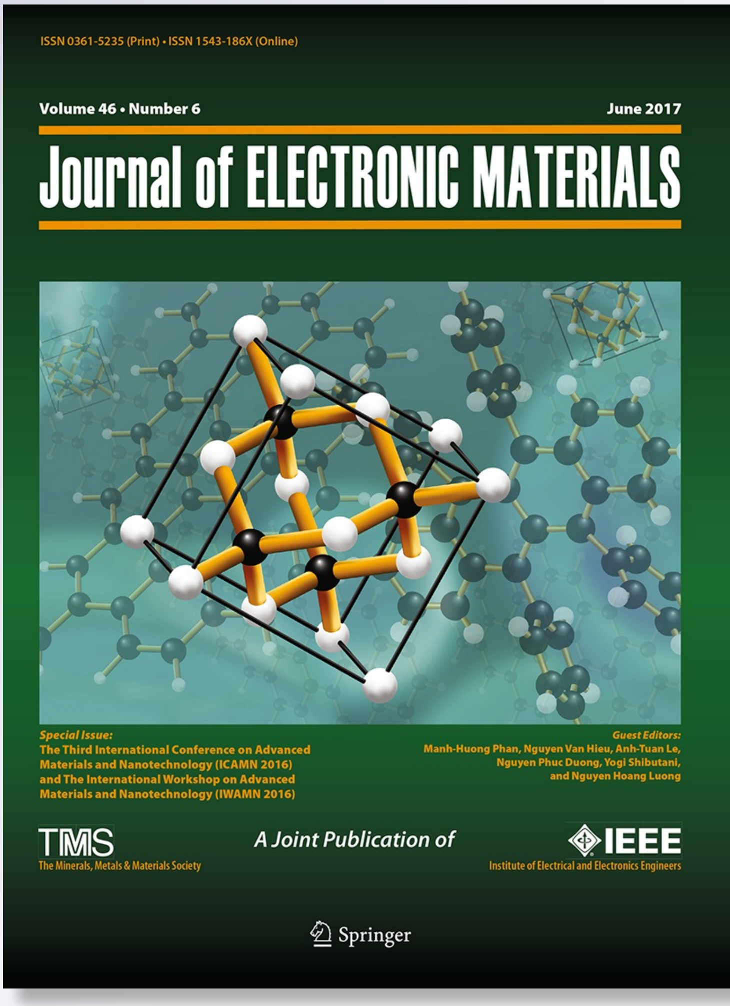

Springer

Journal of ELECTRONIC MATERIALS, Vol. 46, No. 6, 2017
DOI: 10.1007/s11664-017-5396-x

Fabrication by Annealing at Approximately 1030°C and Electrical Characterization of Lead-Free $(1-x)Bi_{0.5}K_{0.5}TiO_3$–$xBa(Fe_{0.5}Nb_{0.5})_{0.05}Ti_{0.95}O_3$ Piezoelectric Ceramics

N. TRUONG-THO[1,3] and N.T. NGHI-NHAN[2]

1.—Department of Physics, College of Sciences, Hue University, 77 Nguyen Hue, Hue, Vietnam. 2.—Department of Physics, College of Sciences, Cheng Kung University, No. 1, University Road, Tainan 701, Taiwan. 3.—e-mail: ntthokh@hueuni.edu.vn

Sintered $(1-x)Bi_{0.5}K_{0.5}TiO_3$–$xBa(Fe_{0.5}Nb_{0.5})_{0.05}Ti_{0.95}O_3$ [(1 − x)BKT–xBFNT] piezoelectric ceramics have been fabricated by conventional annealing at 1000°C to 1050°C. X-ray diffraction (XRD) analysis revealed that the 0.9BKT–0.1BFNT ceramic sintered at 1030°C showed high transition temperature of T_C = 514°C due to presence of $Bi_4Ti_3O_{12}$ in solid solution. Although the *P*–*E* ferroelectric loop was not yet saturated, the remanent polarization and coercive electric field of the 0.9BKT–0.1BFNT showed good values of P_r = 18.5 μC/cm^2 and E_c = 4.3 kV/cm, respectively. The piezoelectric parameters of the ceramic included planar-mode electromechanical coupling factor of k_p = 0.17 and mechanical quality factor of Q_m = 145, larger than the values of 0.17 and 57, respectively, obtained for BKT ceramic.

Key words: Curie temperature, dielectric properties, piezoelectric properties, (1 − x)BKT–xBFNT ceramics

INTRODUCTION

Ferroelectric materials such as $Pb(Zr_{1-x},Ti_x)O_3$ (PZT) have been widely applied because of their exceptional ferroelectric, piezoelectric, and dielectric properties. PZT materials have high Curie temperature for the phase transition ($T_C \approx 193$°C) and large remanent polarization ($P_r \approx 20$ μC/cm^2) corresponding to saturated *P*–*E* hysteresis loops. Due to their excellent piezoelectric properties ($d_{33} \approx 598$ pC/N), these materials have also been used as transducers in ultrasonic and sensor devices.[1,2] However, because of concerns regarding the toxicity of lead oxide, especially at the annealing temperatures used for fabrication of lead-based ceramics, lead-free ferroelectric ceramics have attracted considerable attention in both research and applications.[3,4]

Among the different materials available at present, $Bi_{0.5}K_{0.5}TiO_3$ (BKT) ceramics have been reported to show interesting properties, such as high Curie temperature ($T_C \approx 380$°C) and ferroelectric hysteresis loops that seem well saturated, corresponding to remanent polarization of $P_r \approx$ 35 μC/cm^2 and high depolarization temperature of $T_d \approx 270$°C.[5,6] However, as typical K/Bi-related materials, BKT ceramics show susecptibility to moisture, and their Bi_2O_3 component easily evaporates at high annealing temperature, making fabrication difficult.[7,8] To date, no pure BKT ceramics have shown good piezoelectric properties. To overcome these problem, combination of BKT with $BaTiO_3$ (BT) material, having good dielectric and piezoelectric properties, to form multicomponent ceramics is expected to facilitate fabrication and improve the electrical properties.[9,10]

To improve the physical properties, Nb^{5+} ions can be diffused into BT to increase the grain size and make the as-synthesized ceramics more homogeneous.[11] Simultaneously, introduction of Fe^{3+} ions below 10 mol.% into BT induces a switchable ferroelectric state.[12] Thus, $(1-x)Bi_{0.5}K_{0.5}TiO_3$–

(Received October 12, 2016; accepted February 18, 2017; published online March 6, 2017)

xBa($Fe_{0.5}Nb_{0.5}$)$_{0.05}$$Ti_{0.95}O_3$ ceramics were fabricated and characterized in this study.

EXPERIMENTAL PROCEDURES

The investigated lead-free ceramics have formula $(1-x)Bi_{0.5}K_{0.5}TiO_3$–$x$Ba($Fe_{0.5}Nb_{0.5}$)$_{0.05}$$Ti_{0.95}O_3$ [$(1-x)$BKT–xBFNT] with x = 0.0, 0.05, 0.1, and 0.15. The Bi_2O_3 component is known to evaporate easily at high temperatures, so 20 wt.% Bi_2O_3 must be used to compensate for this effect during fabrication of $(1-x)$BKT–xBFNT.

The starting raw materials were Bi_2O_3, $BaCO_3$, TiO_2, K_2CO_3, Nb_2O_5, and Fe_2O_3 (purity ≥99%). In the first fabrication step, BKT was synthesized from Bi_2O_3, TiO_2, and K_2CO_3. The mixture was milled for 8 h in a PM 400/2 milling machine with zirconia balls and ethanol medium. The powder was then dried, pressed into pellets, and calcined at 850°C for 2 h. In the second step, BFNT was produced from $BaCO_3$, TiO_2, Nb_2O_5, and Fe_2O_3 using the same process as for BKT with sintering temperature of 1200°C for 2 h after milling for 8 h. Finally, the two components (BKT and BFNT) were mixed in various proportions and milled for 8 h for calcination to obtain $(1-x)$BKT–xBFNT powders.

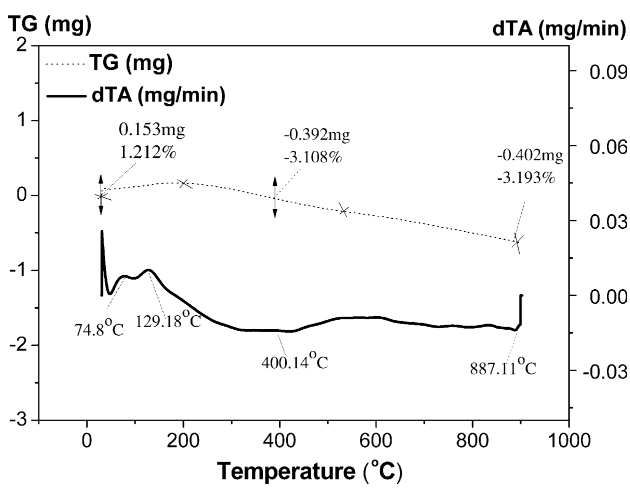

Fig. 1. TG and DTA curves of 0.9BKT–0.1BFNT powder obtained at heating rate of 10°C/min.

The optimal calcination temperature was determined by thermogravimetry (TG) and differential thermal analysis (DTA) of 0.9BKT–0.1BFNT powder. This TG curve indicated that the total mass decreased linearly with increasing temperature. However, an endothermic peak was observed at 887.11°C, indicating that a phase transition occurred in the powder around this temperature. Therefore, the slightly higher temperature of 900°C was set as the calcination temperature to ensure that the phase transition in the sample was complete.

After calcination, each mixture was milled with ethanol medium for 16 h. The powders were then dried and pressed into circular pellets with diameter of 12 mm and thickness of 1.5 mm. The samples were arranged on a crucible and covered with aluminum powder before being sintered at various temperatures of 1000°C, 1030°C, and 1050°C for 2 h.

The bulk density of the sintered samples was measured using the Archimedes method. Their crystal structure was examined by x-ray diffraction (XRD; Rigaku RINT2000) analysis at room temperature. The pellets were poled at 120°C in a silicone oil bath by applying a direct-current (DC) electric field of 30 kV/cm for 20 min. The microstructure of the synthesized samples was analyzed by field-emission scanning electron microscopy (FESEM; JSM-6340F). The dielectric properties were measured as a function of temperature by the resonance and antiresonance frequencies using an impedance analyzer (Agilent 4196B and RLC HIOKI 3532). The ferroelectric properties were measured by applying the Sawyer–Tower method (Fig. 1).

RESULTS AND DISCUSSION

The average grain size was determined from the morphology observed in scanning electron microscopy (SEM) images of the $(1-x)$BKT–xBFNT ceramics with x = 0.05, 0.1, and 0.15 sintered at 1030°C, as shown in Fig. 2. The size of the 0.95BKT–0.05BFNT, 0.9BKT–0.1BFNT, and 0.85BKT–0.15BFNT ceramics sintered at the same temperature of 1030°C was 0.25 μm, 0.31 μm, and 0.27 μm,

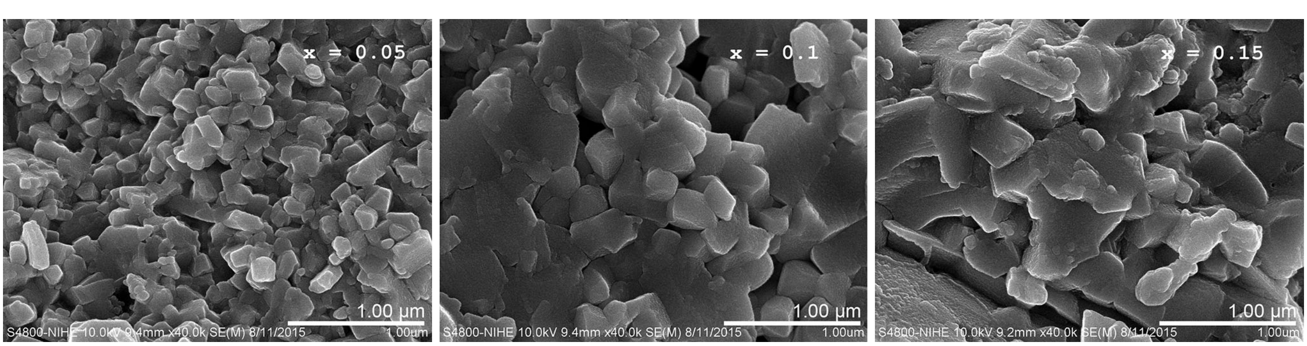

Fig. 2. SEM morphology of $(1-x)$BKT–xBFNT ceramics with x = 0.05, 0.1, and 0.15 sintered at 1030°C.

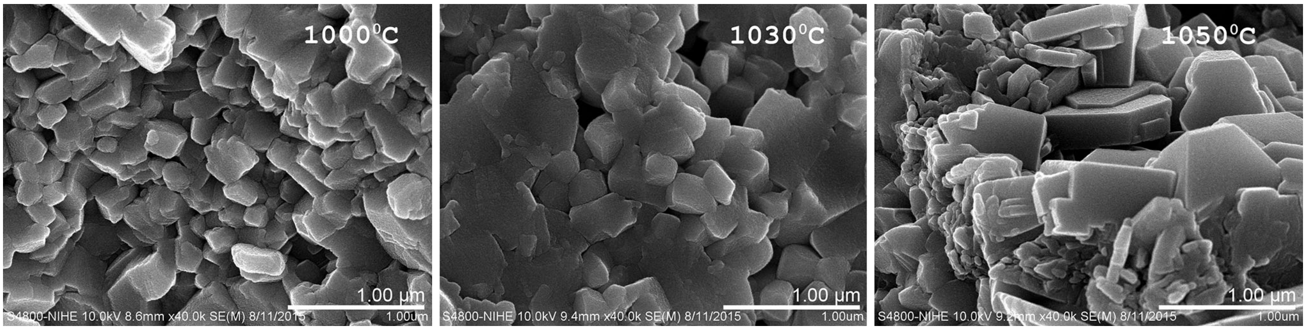

Fig. 3. SEM images of 0.9BKT–0.1BFNT ceramic sintered at 1000°C, 1030°C, and 1050°C.

Table I. Mass density of (1 − x)BKT–xBFNT ceramics sintered at various temperatures

Ceramic	Sintering temperature (°C)	Average mass density (g/cm^3)
0.95BKT–0.05BFNT	1000	5.7
	1030	5.9
	1050	5.6
0.9BKT–0.1BFNT	1000	5.8
	1030	6.1
	1050	5.8
0.85BKT–0.15BFNT	1000	5.9
	1030	5.9
	1050	5.5

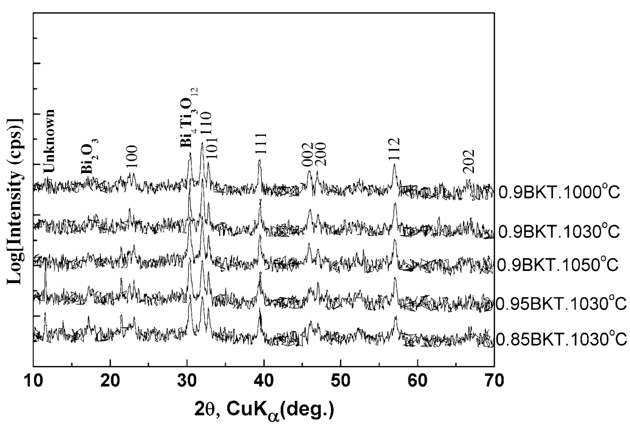

Fig. 4. X-ray diffraction patterns of (1 − x)BKT–xBFNT ceramics.

respectively. Hence, 0.9BKT–0.1BFNT showed the largest grain size amongst the (1 − x)BKT–xBFNT ceramics.

Figure 3 shows the morphology of 0.9BKT–0.1BFNT ceramic sintered at various temperatures. At 1000°C, the grains were small and uniform and had many pores. The density of the samples sintered at this temperature was not high. The sample sintered at 1030°C had grains that were relatively uniform and larger than those of the sample sintered at 1000°C. The grain size seemed to decrease gradually as the sintering temperature was increased to 1050°C. Moreover, the number of pores seemed to increase, whereas the ceramic density decreased to 5.8 g/cm^3.

The mass density of the ceramic products was calculated using the Archimedes principle; the results are presented in Table I, based on which sintering temperature of 1030°C seemed suitable for fabrication of (1 − x)BKT–xBFNT with x = 0.05, 0.1, and 0.15. In particular, the 0.9BKT–0.1BFNT ceramic sintered at 1030°C had mass density of 6.1 g/cm^3.

Figure 4 shows the XRD patterns of the (1 − x)BKT–xBFNT ceramics with x = 0.05, 0.1, and 0.15 annealed at the same temperature of 1030°C. Polycrystalline tetragonal structure of BKT was observed in all of these patterns. The $Bi_4Ti_3O_{12}$ (BIT) peak appeared for all the (1 − x)BKT–xBFNT ceramics. However, the samples with BKT concentration of 0.85 or 0.95 showed some unknown peaks and peaks of monoclinic Bi_2O_3 in orthorhombic phase. These unknown peaks were also found for the 0.9BKT–0.1BFNT ceramic annealed below 1030°C.

Due to the similar ionic radii of Nb^{5+} (0.069 nm), Fe^{3+} (0.0645 nm), and Ti^{4+} (0.0605 nm), substitution of Ti^{4+} by Nb^{5+} and Fe^{3+} may occur in BIT without any peak shifts.[13,14] Estimation of the volume fraction of BKT, BFNT, or/and BIT based on identification of component ions is therefore difficult. In another case, no Bi_2O_3 or unknown peaks appeared. The absence of a Bi_2O_3 peak for the 0.9BKT–0.1BFNT ceramic suggests chemical

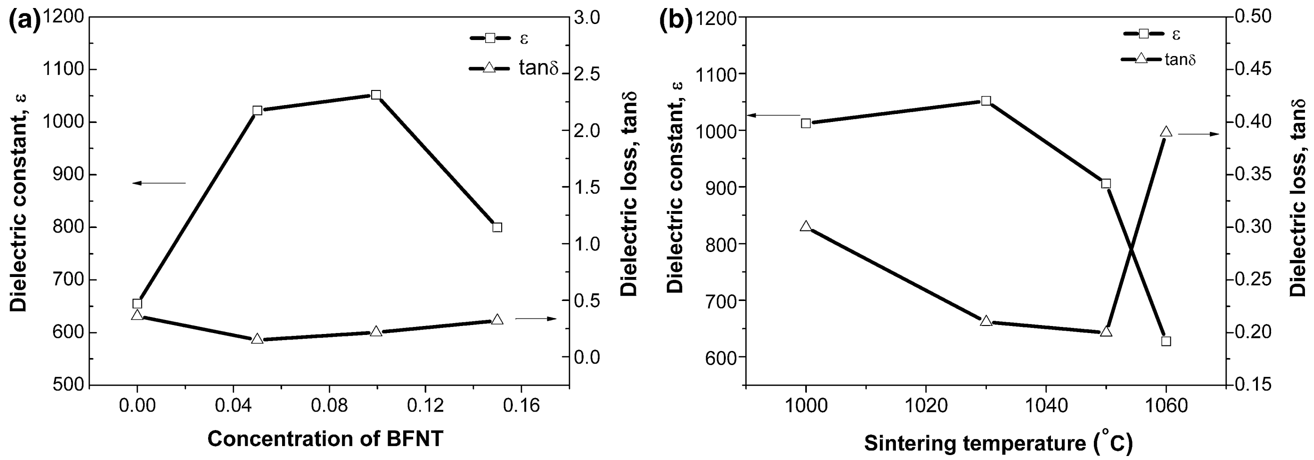

Fig. 5. Dependence of dielectric constant and loss measured at 1 kHz and RT on: (a) the BFNT concentration of (1 − *x*)BKT–*x*BFNT ceramics sintered at 1030°C and (b) the sintering temperature of 0.9BKT–0.1BFNT ceramic.

Table II. Dielectric loss and constant of (1 − *x*)BKT–*x*BFNT ceramics sintered at 1030°C

Ceramic	Thickness (mm)	Diameter (mm)	tan δ	ε
BKT	1.0	10.0	0.36	654.9
0.95BKT–0.05BFNT	1.0	10.0	0.15	1021.9
0.9BKT–0.1BFNT	1.0	10.0	0.21	1051.7
0.85BKT–0.05BFNT	0.9	10.1	0.32	799.7

bonding between Bi_2O_3 and TiO_2 when x was increased from 0 to 0.1, indicating an increase in the volume ratio of BIT to BFNT. Based on this analysis, sintering of 0.9BKT–0.1BFNT at 1030°C may be a suitable fabrication condition for ferroelectric crystallization.

The dielectric properties play an important role in improving the physical characteristics of piezoelectric ceramics. Figure 5a shows the dielectric loss and constant of the (1 − x)BKT–xBFNT ceramics sintered at 1030°C, measured at 1 kHz and room temperature (RT). Table II presents the values of the dielectric properties of the (1 − x)BKT–xBFNT ceramics. The ceramic with $x = 0.9$ exhibited the highest dielectric constant of $\varepsilon = 1052$ and rather low dielectric loss tangent of $\tan\delta = 0.21$. The dielectric loss and constant of the 0.9BKT–0.1BFNT ceramic sintered at various temperatures were also determined and are shown in Fig. 5b. Again, the 0.9BKT–0.1BFNT ceramic sintered at 1030°C showed the highest dielectric constant and low dielectric loss tangent. Presence of Fe^{3+} ions enhances the ferroelectric saturation or/and piezoelectric properties at low concentration. However, an increase in the iron ions leads to a decrease in the dielectric properties.[15,16] In the samples with $x = 0.05$ or 0.15, monoclinic Bi_2O_3 and unknown peaks appeared. When Bi_2O_3 crystallization is enhanced, some Bi_2O_3 clusters might significantly generate conductive spots between metallic electrodes; such spots would prevent poling of the ceramic in physical measurements.[17–19] Therefore, the disappearance of these Bi_2O_3 and unknown peaks corresponded to an improvement in the dielectric properties of the 0.9BKT–0.1BFNT ceramic sintered at 1030°C.

The temperature dependence of the dielectric loss (tan δ) and constant (ε) of the 0.9BKT–0.1BFNT ceramic sintered at 1030°C was investigated and is shown in Fig. 6. The dielectric constant was found to increase as the temperature was increased, peaking at 514°C and decreasing thereafter. Thus, the Curie temperature of the 0.9BKT–0.1BFNT ceramic was 514°C, higher than the values of 380°C and 120°C for $(Bi_{0.5}K_{0.5})TiO_3$ and $BaTiO_3$, respectively.[5,10] Thus, we suppose that there is a component having Curie temperature above 514°C in the 0.9BKT–0.1BFNT sample. This means that the ceramic product contained not only $(Bi_{0.5}K_{0.5})TiO_3$ and $BaTiO_3$ with Curie temperature below 514°C but also a compound having Curie temperature above 514°C. Having Curie temperature of 675°C, presence of $Bi_4Ti_3O_{12}$ is reasonable, as also indicated by the appearance of the corresponding peak in the XRD pattern.[18]

The *P*–*E* hysteresis loops of the (1 − x)BKT–xBFNT ceramics sintered at 1030°C were measured at RT using the Sawyer–Tower method and are shown in Fig. 7; the remanent polarization P_r and coercive field E_c were also determined and are shown in Fig. 8. Undoped BKT and 0.85BKT–0.15BFNT ceramics showed leaky *P*–*E* hysteresis

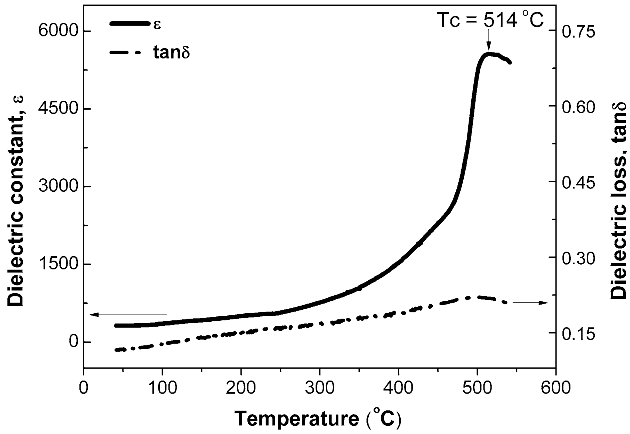

Fig. 6. Temperature dependence of dielectric constant (ε) and dielectric loss (tan δ) of 0.9BKT–0.1BFNT ceramic sintered at 1030°C.

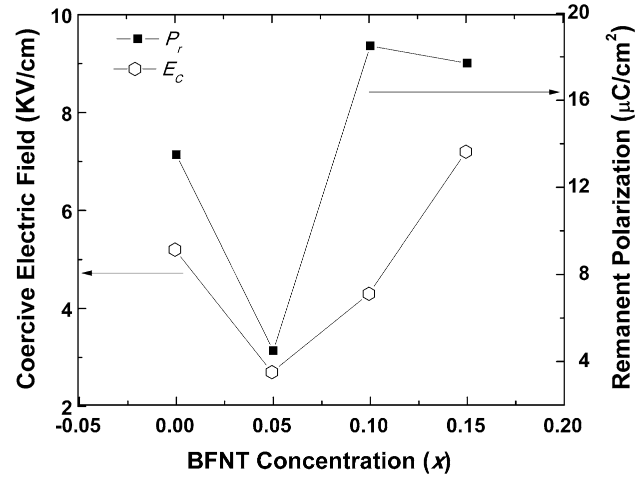

Fig. 8. Remanent polarization and coercive electric field of (1 – x)BKT–xBFNT ceramics sintered at 1030°C.

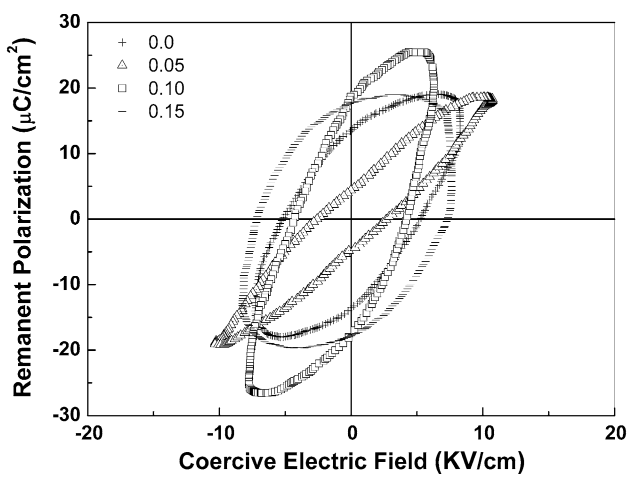

Fig. 7. *P–E* hysteresis loops of (1 – x)BKT–xBFNT ceramics sintered at 1030°C with $x = 0$, 0.05, 0.1, and 0.15, measured at RT.

loops, the shapes of which were not the classical ferroelectric type. The loop of the 0.95BKT–0.05BFNT ceramic was narrow. Thus, although the coercive electric field was low at 2.7 kV/cm, the polarization at zero field was only 4.5 $\mu C/cm^2$. On the other hand, the *P–E* hysteresis loop of the 0.9BKT–0.1BFNT ceramic showed good ferroelectric properties, with high polarization of $P_r = 18.5\ \mu C/cm^2$ and rather low coercive electric field of $E_c = 4.3$ kV/cm.

The ferroelectric properties of the $(1-x)$BKT–xBFNT samples can be understood based on analysis of the role of BFNT in the as-synthesized ceramics. When increasing x from 0 to 0.1, the appearance of BIT, a ferroelectric material, and the decrease of the intensity of Bi_2O_3 peaks in the XRD patterns will correspond to improved ferroelectric and dielectric properties of the $(1-x)$BKT–xBFNT ceramics sintered at 1030°C.[7,8] Therefore, the narrow hysteresis loop can be explained by the slight improvement in the dielectric properties when $x = 0.05$. The improvement of the ferroelectric properties can be explained based on the role of BFNT as a catalyst for generation of BIT in the $(1-x)$BKT–xBFNT ceramics. When $x = 0.1$, the combination of Bi_2O_3 and TiO_2 into BIT is saturated. As a result, the largest values of $P_r = 18.5\ \mu C/cm^2$ for the remanent polarization and $E_c = 4.3$ kV/cm for the coercive electric field were obtained for the 0.9BKT–0.1BFNT ceramic. On the other hand, when x was increased above 0.1, the BIT and unknown peaks reappeared in the XRD pattern (Fig. 4), corresponding to suppressed dielectric properties. Thus, the 0.85BKT–0.15BFNT ceramic was highly leaky, and the *P–E* hysteresis loops became similar to those of undoped BKT ceramic.

The ceramic was shaped like a thin disc, thus both the planar-mode electromechanical coupling factor k_p and the mechanical quality factor Q_m of the $(1-x)$BKT–xBFNT ceramics sintered at 1030°C were calculated from the frequency dependence of the impedance Z obtained at RT, as shown in Fig. 9.[20] Table III presents the values of k_p, Q_m, and the minimum impedance Z_m measured at RT for the $(1-x)$BKT–xBFNT ceramics sintered at 1030°C with $x = 0$ to 0.15. The obtained values of k_p, Q_m, and $Z_m(\Omega)$ for pure BKT ceramic were 1002, 0.17, and 57, respectively. For the samples with $x = 0.05$ or 0.15, although the minimum impedance Z_m was improved, the piezoelectric properties, such as k_p and Q_m, were still suppressed due to the limitation of the dielectric properties. On the other hand, 0.9BKT–0.1BFNT showed the highest electromechanical coupling factor ($k_p = 0.21$) and mechanical quality factor ($Q_m = 145$) and lowest minimum impedance ($Z_m = 317\ \Omega$). As mentioned above, the increasing volume ratio of BIT to BT as x was increased from 0 to 0.1 decreased the content of Bi_2O_3 and other unknown materials. Therefore, the physical characteristics, including the ferroelectric

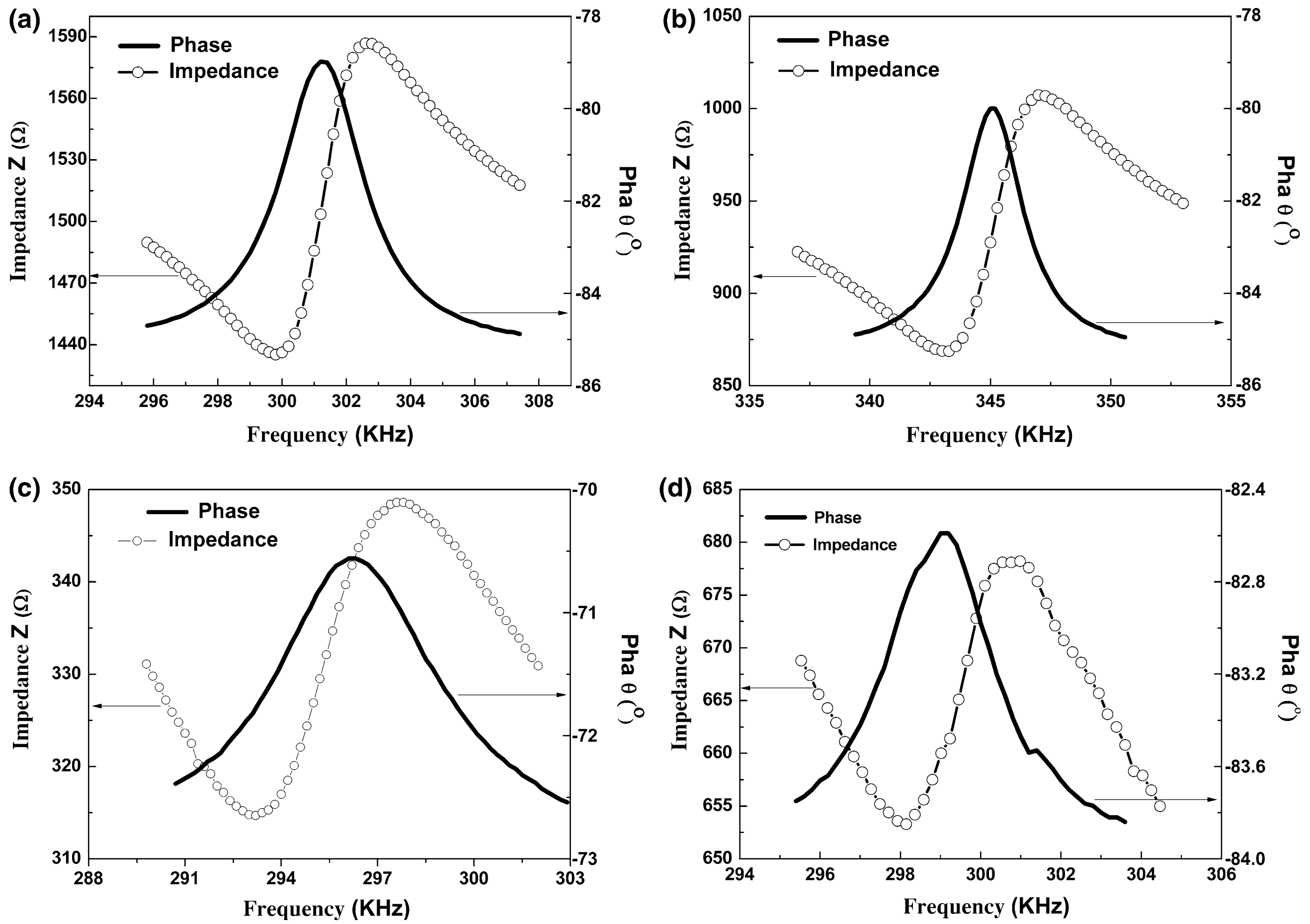

Fig. 9. Frequency dependence of impedance Z and phase θ of (a) BKT, (b) 0.95BKT–0.05BFNT, (c) 0.9BKT–0.1BFNT, and (d) 0.85BKT–0.15BFNT ceramics sintered at 1030°C.

Table III. Minimum impedance (Z_m), electromechanical coupling factor (k_p), and mechanical quality factor (Q_m) of (1 − x)BKT–xBFNT ceramics

Ceramic	Z_{min} (Ω)	K_p	Q_m
BKT	1002	0.17	57
0.95BKT–0.05BFNT	825	0.15	62
0.9BKT–0.1BFNT	317	0.21	145
0.85BKT–0.15BFNT	638	0.15	104

and piezoelectric properties, of the 0.9BKT–0.1BFNT ceramic sintered at 1030°C were improved. When x was increased above 0.1, the Bi_2O_3–TiO_2 chemical bonding in BIT crystals was gradually broken down. This phenomenon led to a decrease in the dielectric and piezoelectric properties.

CONCLUSIONS

We fabricated $(1-x)Bi_{0.5}K_{0.5}TiO_3$–$xBa(Fe_{0.5}Nb_{0.5})_{0.05}Ti_{0.95}O_3$ ceramics with x = 0.0, 0.05, 0.1, and 0.15 by conventional annealing at various temperatures from 1000°C to 1050°C. XRD analysis clearly revealed perovskite phase with tetragonal BKT ceramic structure, as well as a $Bi_4Ti_3O_{12}$ peak. The (1 − x)BKT–xBFNT ceramics sintered at 1030°C showed high mass density. Meanwhile, the morphology of 0.9BKT–0.1BFNT sintered at 1030°C showed the largest grain size and mass density. In particular, the Curie temperature of the ceramic was 514°C due to presence of $Bi_4Ti_3O_{12}$ in the solid system. At RT, the P–E hysteresis loops of $(1-x)Bi_{0.5}K_{0.5}TiO_3$–$xBa(Fe_{0.5}Nb_{0.5})_{0.05}Ti_{0.95}O_3$ ceramics sintered at 1030°C were observed. Although the loop was still not saturated, the remanent polarization and coercive electric field of 0.9BKT–0.1BFNT showed good values of P_r = 18.5 $\mu C/cm^2$ and E_c = 4.3 kV/cm, respectively. Some piezoelectric parameters of the $(1-x)Bi_{0.5}K_{0.5}TiO_3$–$xBa(Fe_{0.5}Nb_{0.5})_{0.05}Ti_{0.95}O_3$ ceramics sintered at 1030°C were obtained, namely the planar-mode electromechanical coupling factor (k_p) and mechanical quality factor (Q_m) at RT. Among the investigated ceramics, 0.9BKT–0.1BFNT sintered at 1030°C also showed good piezoelectric properties with k_p = 0.17 and Q_m = 145, improved compared with those of BKT ceramic.

ACKNOWLEDGEMENT

This research was funded by the Vietnam National Foundation for Science and Technology Development (NAFOSTED) under Grant No. 103.02-2015.66.

REFERENCES

1. B. Jafe, W. Cook, and H. Jafe, eds., *Piezoelectric Ceramics* (New York: Academic, 1971).
2. Y. Xu, *Ferroelectric Materials and Their Applications* (Amsterdam: Elsevier Science, 1991).
3. N.T. Tho, A. Inoue, M. Noda, and M. Okuyama, *IEEE Trans. Ultrason. Ferroelectr. Freq. Control* 54, 2603 (2007).
4. L. Simon-Seveyrat, A. Hajjaji, Y. Emziane, B. Guiffard, and D. Guyomar, *Ceram. Int.* 33, 35 (2007).
5. C.F. Buhrer, *J. Chem. Phys.* 36, 798 (1962).
6. K. Tabuchi, H. Nagata, and T. Takenaka, *J. Ceram. Soc. Jpn.* 121, 623 (2013).
7. J. König, M. Spreitzer, B. Jancar, D. Suvorov, Z. Samardzija, and A. Popovic, *J. Eur. Ceram. Soc.* 29, 1695 (2009).
8. T. Wada, A. Fukui, and Y. Matsuo, *Jpn. J. Appl. Phys.* 41, 7025 (2002).
9. H. Takahashi, Y. Numamoto, J. Tani, K. Matsuta, J. Qiu, and S. Tsurekawa, *Jpn. J. Appl. Phys.* 45, L30 (2006).
10. M.M. Vijatovic, J.D. Bobic, and B.D. Stojanovic, *Sci. Sinter.* 40, 235 (2008).
11. W.R. Buessem and M. Kahn, *J. Am. Ceram. Soc.* 54, 458 (1971).
12. E.V. Ramana, S.M. Yang, R. Jung, M.H. Jung, B.W. Lee, and C.U. Jung, *J. Appl. Phys.* 113, 187219 (2013).
13. H. Shulman, D. Damjanovic, and N. Setter, *J. Am. Ceram. Soc.* 83, 528 (2000).
14. X.Q. Chen, F.J. Yang, W.Q. Cao, H. Wang, C.P. Yang, D.Y. Wang, and K. Chen, *Solid State Commun.* 150, 1221 (2010).
15. K. Fukai, K. Hidaka, M. Aoki, and K. Abe, *Ceram. Int.* 16, 285 (1990).
16. G. Arlt, D. Henningsand, and G. deWith, *J. Appl. Phys.* 58, 1619 (1985).
17. H. Bea, M. Bibes, A. Barthelemy, K. Bouzehouane, E. Jacquet, A. Khodan, J.P. Contour, S. Fusil, F. Wyczisk, A. Forget, D. Lebeugle, D. Colson, and M. Viret, *Appl. Phys. Lett.* 87, 072508 (2005).
18. N. Truong Tho, T. Kanashima, and M. Okuyama, *Jpn. J. Appl. Phys.* 49, 095803 (2010).
19. N. Truong Tho, T. Kanashima, M. Sohgawa, D. Ricinschi, M. Noda, and M. Okuyama, *Jpn. J. Appl. Phys.* 49, 5 (2010).
20. IRE Standards on Piezoelectric, *IEEE Standard 179-1961* (New York: Institute of Electrical and Electronic Engineers, 1961).